

## Wavelength-shifting fiber signal readout from Transparent RUBber SheeT (TRUST) type LiCaAlF<sub>6</sub> neutron scintillator

Watanabe, Kenichi  
Graduate School of Engineering, Nagoya University

Yamazaki, Takuya  
Graduate School of Engineering, Nagoya University

Sugimoto, Dai  
Graduate School of Engineering, Nagoya University

Yamazaki, Atsushi  
Graduate School of Engineering, Nagoya University

他

<https://hdl.handle.net/2324/7168651>

---

出版情報 : Nuclear Instruments and Methods in Physics Research Section A: Accelerators,  
Spectrometers, Detectors and Associated Equipment. 784, pp.260-263, 2015-06-01. Elsevier  
バージョン :  
権利関係 :



**Wavelength-shifting fiber signal readout from  
Transparent Rubber SheeT (TRUST) type LiCaAlF<sub>6</sub> neutron scintillator**

Kenichi Watanabe<sup>1</sup>, Takuya Yamazaki<sup>1</sup>, Dai Sugimoto<sup>1</sup>, Atsushi Yamazaki<sup>1</sup>, Akira Uritani<sup>1</sup>, Tetsuo Iguchi<sup>1</sup>,  
Kentaro Fukuda<sup>2</sup>, Sumito Ishidu<sup>2</sup>, Takayuki Yanagida<sup>3</sup>, Yutaka Fujimoto<sup>3</sup>

<sup>1</sup> Graduate School of Engineering, Nagoya University, Nagoya, 464-8603, Japan

<sup>2</sup> Tokuyama Corporation, Shunan, 745-8648, Japan

<sup>3</sup> Kyushu Institute of Technology, Kita-kyushu, 808-0196, Japan

Corresponding author: Kenichi Watanabe, Nagoya University

Tel: +81-52-789-4513, Fax.: +81-52-789-3843

E-mail: k-watanabe@nucl.nagoya-u.ac.jp

**Abstract**

As an alternative to the standard <sup>3</sup>He neutron detector, we are developing the Transparent Rubber SheeT type (TRUST) Eu doped LiCaAlF<sub>6</sub> (Eu:LiCAF) scintillator. This type of neutron scintillator can easily be fabricated as a large area sheet. In order to take advantage of a large area detector, we try to readout scintillation photons using a wavelength-shifting fiber (WLSF) from a TRUST Eu:LiCAF scintillator. The TRUST Eu:LiCAF scintillator with the size of 50x50x5 mm<sup>3</sup> was mounted on the WLSF plate and the end of the WLSFs was connected with a PMT. In order to reject high pulse height events induced in the WLSFs, we applied the pulse shape discrimination technique. The gamma-ray intrinsic and neutron absolute detection efficiency is evaluated to be 8.8x10<sup>-7</sup> and 9x10<sup>-3</sup> cps/ng Cf (2m) for the TRUST Eu:LiCAF scintillator with the size of 50x50x5 mm<sup>3</sup>.

**KEYWORDS:** <sup>3</sup>He alternatives, neutron detector, TRUST Eu:LiCAF., neutron scintillator

## 1. Introduction

Neutron detection techniques play an important role in various fields such as homeland security, nuclear safeguards, non-destructive test etc. For thermal neutron detection, a  $^3\text{He}$  proportional counter has been used as the gold standard detector. However, worldwide  $^3\text{He}$  gas shortage is recently a severe problem [1-2]. Therefore, alternatives to the conventional  $^3\text{He}$  neutron detectors have been required to be developed. Alternatives to  $^3\text{He}$  counter must have sufficiently high detection efficiency and good gamma-ray rejection ability. Although a  $\text{BF}_3$  gas counter is one of the alternatives, it should be taken care on its toxicity and requires relatively high bias voltage due to its poor charge collection [2]. Boron-lined proportional counters can also be promising candidates [3]. The detection efficiency of this type of detector is limited by the thickness of boron coating. For applications requiring high detection efficiency, a lot of narrow tubes must be arranged. Inorganic scintillators containing  $^6\text{Li}$  or  $^{10}\text{B}$ , which have high neutron absorption cross section, have also ability of thermal neutron detection. Solid phase scintillator can contain much greater number of  $^6\text{Li}$  or  $^{10}\text{B}$  atoms than  $^3\text{He}$  gas counter. However, they usually suffer from interference of gamma-ray. As one of the promising candidates, we are developing  $\text{LiCaAlF}_6$  (LiCAF) scintillators [4-8]. Two types of LiCAF scintillators, Ce and Eu doped LiCAF (Ce:LiCAF and Eu:LiCAF), can be used. Both scintillators have relatively high light yield, light composition, high transparency and no hygroscopicity. These scintillators can show clear neutron absorption peak in the pulse height spectrum due to its high transparency. Since Ce:LiCAF scintillator additionally have relatively high  $\alpha/\beta$  ratio and ability of pulse shape discrimination between neutron and gamma-ray, they can efficiently reject gamma-ray events [4][7-8]. However, its emission wavelength is 285 nm, where the quantum efficiency of a common photomultiplier tube (PMT) is not so high, and its light yield is one-fifth of Eu:LiCAF. In order to effectively use Ce:LiCAF scintillator, we should use a high performance PMT, which is usually expensive. On the other hand, Eu:LiCAF scintillator has adequate emission wavelength of 375 nm and much higher light yield than Ce:LiCAF. However, Eu:LiCAF strongly suffers from gamma-ray interference because of its relatively low  $\alpha/\beta$  ratio [5-6]. For high detection efficiency, a large size crystal is required but a large crystal growth imposes relatively long growth time and high cost. As a solution of these problems, we have developed a

Transparent Rubber Sheet Type (TRUST) Eu:LiCAF scintillator. This type of scintillator has good gamma-ray rejection ability while keeping sufficiently high detection efficiency. In addition, this scintillator is flexible sheet and can be fabricated into large size sheet easily. In order to take advantage of the geometrical flexibility, we try to readout scintillation photons using a wavelength-shifting fiber (WLSF) from a TRUST Eu:LiCAF scintillator.

## **2. TRUST Eu:LiCAF scintillator**

As mentioned above, Eu:LiCAF scintillator has excellent properties for neutron detection such as significant light yield, adequate emission wavelength and high transparency. Although this scintillator can show clear neutron absorption peak in the pulse height spectrum, its low  $\alpha/\beta$  ratio leads to significant interference from gamma rays with high energy of MeV order. In order to reduce interference of gamma rays, controlling the size of scintillators is useful. When scintillator size is controlled smaller than the range of fast electrons induced by gamma rays but larger than the range of reaction products in  ${}^6\text{Li}(n,t)\alpha$  reactions, signal pulse height can selectively be reduced only for gamma-ray induced events. Under this situation, neutron induced events can show a clear peak in the pulse height spectrum. Consequently, a small piece of Eu:LiCAF scintillator can easily discriminate neutron and gamma-ray events with the signal pulse height.

A small piece scintillator inevitably has quite small neutron detection efficiency. In order to increase the detection efficiency with the gamma-ray rejection ability, a large number of small pieces of scintillators must be arranged over a sensitive area of a photo detector. This configuration is difficult to achieve uniform collection of scintillation photons because small pieces are difficult to be fabricated with uniform size and shape. In order to achieve uniform light collection from small pieces of scintillators, we propose to disperse small pieces into transparent rubber with a similar refractive index, which can suppress refractions and reflections on interfaces between the scintillators and the rubber, and to form the rubber into a sheet shape. In this configuration, a large number of small scintillator pieces can be arranged with uniform light collection efficiency. This type of neutron scintillator is referred to as TRUST Eu:LiCAF scintillator.

**Figure 1** shows a photograph of TRUST Eu:LiCAF scintillator. A bulk scintillator of the Eu:LiCAF single crystal (bulk Eu:LiCAF) is also shown in this photograph. This scintillator has both relatively high neutron sensitivity and high gamma-ray suppression ability. **Figure 2** shows pulse height spectrum obtained from the TRUST Eu:LiCAF scintillator. Pulse height spectrum obtained from a bulk Eu:LiCAF scintillator is also shown in **Fig. 2**. In these measurements, the scintillators were directly mounted on the PMT photocathode window and the lower level discrimination of the multi-channel analyzer (MCA) was not same for both measurements. In TRUST Eu:LiCAF scintillator, pulse heights can selectively be reduced only for gamma-ray events compared with the bulk Eu:LiCAF. In this configuration, the density of dispersed small scintillators is important parameter. If we densely disperse small pieces of Eu:LiCAF scintillators into a transparent rubber sheet, gamma-ray rejection ability is deteriorated because fast electrons induced by gamma rays can re-enter into neighbor scintillators.

This rubber sheet is, additionally, flexible and allows easy handling compared with single crystal or glass scintillators, which are fragile and require delicate handling. The TRUST Eu:LiCAF scintillator can be fabricated into large size sheet easily. In order to take advantage of the geometrical flexibility, WLSF readout of scintillation photons is quite desirable. The WLSF can absorb scintillation photons from a fiber side surface and re-emits photons, which are wavelength-shifted to longer wavelength, into the fiber core. These wavelength-shifted photons can be transmitted along the fiber and detected with a PMT at the fiber end. Therefore, WLSF readout is suitable for scintillation photon collection from a large area scintillator.

### 3 Experiments

In order to perform the WLSF readout, the WLSF array plate, in which 36 WLSFs with 1 mm diameter and more than 20cm length were arranged with 1.5 mm pitch into plate shape, was fabricated. The TRUST Eu:LiCAF scintillator with the size of 50x50x5 mm<sup>3</sup> was mounted on the WLSF plate. The ends of WLSFs were bundled and connected into a PMT, Hamamatsu R7600U. The detector configuration is shown in **Fig. 3**. The scintillator was wrapped with a polytetrafluoroethylene (PTFE) sheet, except for a

1 surface contacting the WLSF plate, as a reflector. The whole detector unit was shielded with a black sheet  
2 from an ambient light.

3 The detector was irradiated with  $^{252}\text{Cf}$  neutron source or  $^{60}\text{Co}$  gamma-ray source for response  
4 evaluation. The PMT anode signal was fed into a shaping amplifier (ORTEC 571) through a preamplifier  
5 (ORTEC 113). The amplitude of shaped pulses was digitized with an analog-to digital converter (ADC).  
6 The pulse height spectra were created with a MCA (Fast COMTEC, MPA-3) and were shown on a personal  
7 computer.

8 Gamma rays and neutrons can directly interact in WLSFs. These interaction events can produce  
9 undesirable noise signal. In order to distinguish scintillation events in TRUST Eu:LiCAF scintillator with  
10 ones in WLSFs, the pulse shape discrimination technique can be applied. **Figure 4** shows examples of  
11 signal waveforms created in the TRUST Eu:LiCAF scintillator and the WLSFs. The decay time of  
12 scintillation pulses induced in the TRUST Eu:LiCAF and the WLSFs are a few  $\mu\text{s}$  and a few ns, respectively.  
13 In order to discriminate each event, we applied the dual shaping time method. Output signals from the  
14 preamplifier were split into two shaping amplifiers with different shaping time. Fast and slow shaping time  
15 were set to 0.5  $\mu\text{s}$  and 3  $\mu\text{s}$ , respectively. Two shaped pulses were simultaneously digitized and analyzed  
16 with multi-parameter MCA (Fast COMTEC, MPA-3).

17 We also evaluated the neutron absolute detection efficiency and the gamma-ray intrinsic detection  
18 efficiency. When measuring the neutron absolute detection efficiency, a  $^{252}\text{Cf}$  neutron source with  $2.1 \times 10^5$   
19 n/s, corresponding to 92 ng Cf, was placed at a distance of 2 m from the detector surface. The Cf source  
20 was surrounded with 5 mm thick lead and 25 mm thick polyethylene moderator. For evaluation of  
21 gamma-ray intrinsic detection efficiency, a  $^{60}\text{Co}$  gamma-ray source with  $2.4 \times 10^5$  Bq was placed at a distance  
22 of 10 cm from the detector surface.

## 23 24 25 **4 Results and Discussion**

26 **Figure 5** shows pulse height spectra obtained from the TRUST Eu:LiCAF scintillator with the

WLSF readout. The spectrum obtained from only the WLSF plate is also plotted. Gamma-ray induced events have relatively high pulse height and interfere in the neutron peak region unlike the direct readout case. The spectrum obtained from the WLSF plate without a TRUST Eu:LiCAF scintillator is almost the same as one obtained with TRUST Eu:LiCAF scintillator. This implies that these events with relatively high pulse height is induced in the WLSF plate. The WLSF is almost a plastic scintillation fiber. They have quite fast scintillation decay time of a few ns. On the other hand, the TRUST Eu:LiCAF scintillator has relatively slow decay time of a few  $\mu$ s. We can discriminate each event using the pulse shape discrimination technique. We applied the dual shaping time method. **Figure 6** shows two dimensional histogram between pulse heights of shaped pulses with slow (3  $\mu$ s) and fast (0.5  $\mu$ s) shaping time. Events induced in the WLSFs can be distinguished from ones induced in TRUST Eu:LiCAF scintillator clearly. We can easily reject the WLSF events from the TRUST Eu:LiCAF events by using the ratio between pulse heights of shaped pulses with fast and slow shaping time. **Figure 7** shows pulse height spectra obtained from the TRUST Eu:LiCAF scintillator with the WLSF readout, when applying the pulse shape discrimination. High pulse height component induced in the WLSFs is confirmed to be suppressed. A little of high pulse height events still remain. Since these events also stay in back ground measurement, they are considered to be cosmic muon induced events.

Finally, we evaluated the gamma-ray intrinsic and the neutron absolute detection efficiency. The gamma-ray intrinsic detection efficiency for  $^{60}\text{Co}$  gamma rays is evaluated to be  $8.8 \times 10^{-7}$ . The neutron absolute detection efficiency of the TRUST Eu:LiCAF scintillator with the size of  $50 \times 50 \times 5 \text{ mm}^3$  is evaluated to be  $9 \times 10^{-3} \text{ cps/ng Cf}$  when placing the  $^{252}\text{Cf}$  source at 2 m away from the detector surface. In order to achieve 2.5 cps/ng Cf (2m), the size of the TRUST Eu:LiCAF scintillator should be  $200 \times 850 \times 20 \text{ mm}^3$ .

## 5. Conclusion

We are developing the large area neutron detector using the TRUST Eu:LiCAF scintillator with the WLSF readout. We fabricated the WLSF readout unit for TRUST Eu:LiCAF scintillator and

evaluated the response of the fabricated detector. Events induced in the WLSFs have relatively high pulse height and interfere in the neutron absorption peak region. The pulse shape discrimination technique is useful to reject the events induced in the WLSFs. We, consequently, evaluate the gamma-ray intrinsic and the neutron absolute detection efficiency. The gamma-ray intrinsic and the neutron absolute detection efficiency are evaluated to be  $8.8 \times 10^{-7}$  and  $9 \times 10^{-3}$  cps/ng Cf (2m) for the TRUST Eu:LiCAF scintillator with the size of  $50 \times 50 \times 5$  mm<sup>3</sup>. When using the TRUST Eu:LiCAF scintillator of  $200 \times 850 \times 20$  mm<sup>3</sup> size, we can achieve 2.5 cps/ng Cf.

## Acknowledgements

This study is the result of "Development of an alternative to He-3 neutron detectors for homeland security and nuclear material safeguards" carried out under the Adaptable and Seamless Technology transfer Program through targetdrive R&D by Japan Science and Technology Agency.

## References

- [1] R.T. Kouzes, The <sup>3</sup>He Supply Problem, PNNL-18388 (2009)
- [2] R. T. Kouzes, J. H. Ely, L. E. Erikson, W. J. Kernan, A. T. Lintereur, E. R. Siciliano, D. L. Stephens, D. C. Stromswold, R. M. V. Ginhoven, M. L. Woodring, Neutron detection alternatives to <sup>3</sup>He for national security applications, Nuclear Instruments and Methods in Physics Research Section A, **623**, 1035-1045 (2010)
- [3] A. T. Lintereur, R. T. Kouzes, J. H. Ely, L. E. Erikson, E. R. Siciliano, M. L. Woodring, Boron-lined neutron detector measurements, PNNL-18938 (2009)
- [4] A. Yoshikawa, T. Yanagida, Y. Yokota, N. Kawaguchi, S. Ishizu, K. Fukuda, T. Suyama, K. J. Kim, J. Pejchal, M. Nikl, K. Watanabe, M. Miyake, M. Baba, K. Kamada, Single Crystal Growth, Optical Properties and Neutron Response of Ce<sup>3+</sup> Doped LiCaAlF<sub>6</sub>, IEEE Transactions on Nuclear Science, **56**, 3796-3799 (2009)



- [5] T. Yanagida, N. Kawaguchi, Y. Fujimoto, K. Fukuda, Y. Yokota, A. Yamazaki, K. Watanabe, J. Pejchal, A. Uritani, T. Iguchi, A. Yoshikawa, Basic study of Europium doped LiCaAlF<sub>6</sub> scintillator and its capability for thermal neutron imaging application, *Optical Materials*, **33**, 1243-1247 (2011)
- [6] T. Yanagida, A. Yamaji, N. Kawaguchi, Y. Fujimoto, K. Fukuda, S. Kurosawa, A. Yamazaki, K. Watanabe, Y. Futami, Y. Yokota, A. Uritani, T. Iguchi, A. Yoshikawa, M. Nikl, Europium and Sodium Codoped LiCaAlF<sub>6</sub> Scintillator for Neutron Detection, *Applied Physics Express*, **4**, 106401 (2011)
- [7] A. Yamazaki, K. Watanabe, A. Uritani, T. Iguchi, N. Kawaguchi, T. Yanagida, Y. Fujimoto, Y. Yokota, K. Kamada, K. Fukuda, T. Suyama, A. Yoshikawa, Neutron-gamma discrimination based on pulse shape discrimination in a Ce:LiCaAlF<sub>6</sub> scintillator, *Nuclear Instruments and Methods in Physics Research Section A*, **652**, 435-438 (2011)
- [8] K. Watanabe, Y. Kondo, A. Yamazaki, A. Uritani, T. Iguchi, N. Kawaguchi, K. Fukuda, S. Ishidu, T. Yanagida, Y. Fujimoto, A. Yoshikawa, Temperature Dependence of Neutron-Gamma Discrimination Based on Pulse Shape Discrimination Technique in a Ce:LiCaAlF<sub>6</sub> Scintillator, *IEEE Transactions on Nuclear Science*, **60**, 959-962 (2013)

## Figure Captions

**Figure 1** Photograph of TRUST and bulk Eu:LiCAF.

**Figure 2** Pulse height spectra obtained from a) bulk Eu:LiCAF and b) TRUST Eu:LiCAF.

**Figure 3** Dependence of dosimeter signal intensity on the setting position depth obtained from basic experiments.

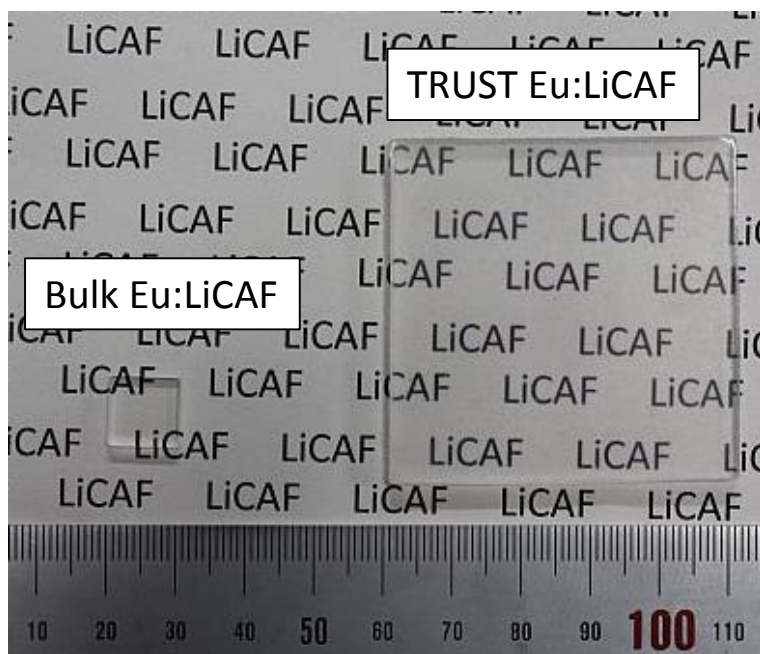
**Figure 4** Signal waveforms created in the TRUST Eu:LiCAF scintillator and the WLSFs.

**Figure 5** Pulse height spectra obtained from the TRUST Eu:LiCAF scintillator with the WLSF readout. The spectra obtained from only the WLSF plate is also plotted.

**Figure 6** Two dimensional histogram between pulse heights of shaped pulses with slow (3  $\mu$ s) and fast (0.5  $\mu$ s) shaping time.

**Figure 7** Pulse height spectra obtained from the TRUST Eu:LiCAF scintillator with the WLSF readout, when applying the pulse shape discrimination.

1



2

3

4

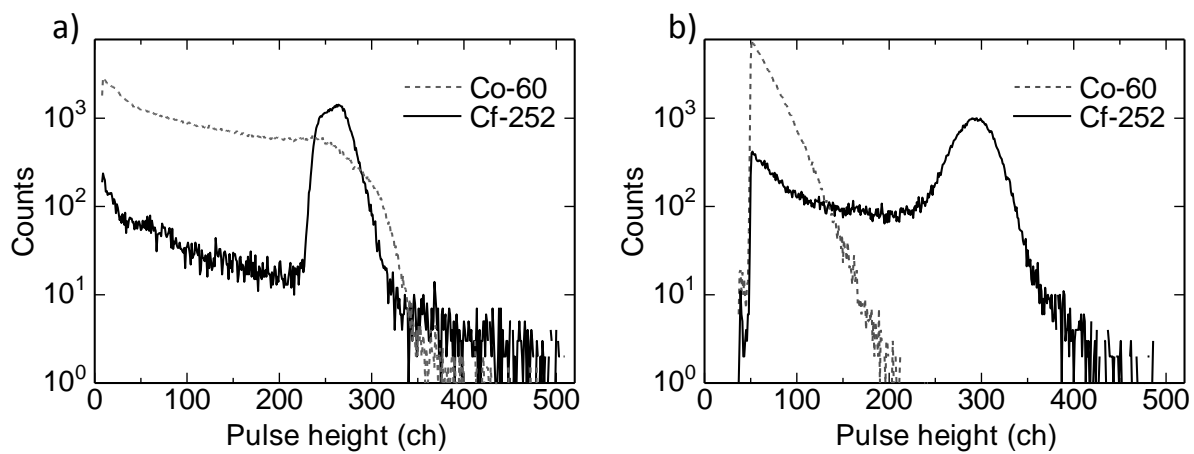
5 **Figure 1** Photograph of TRUST and bulk Eu:LiCAF.

6

7

8

1



2

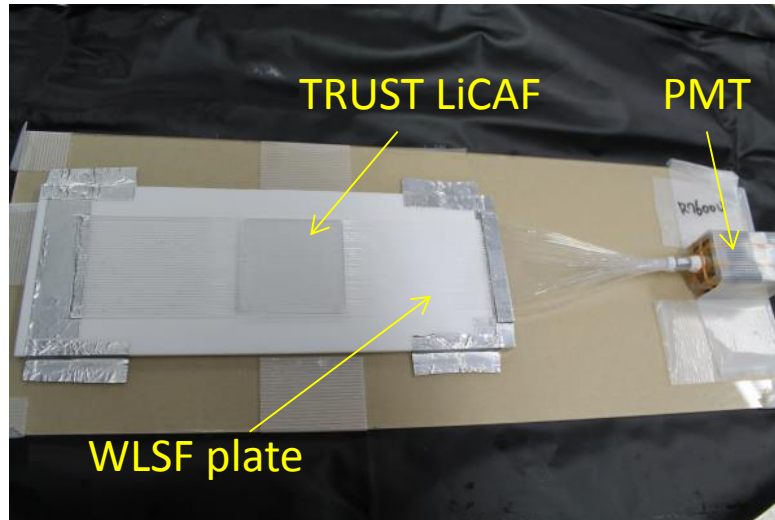
3

4 **Figure 2** Pulse height spectra obtained from a) bulk Eu:LiCAF and b) TRUST Eu:LiCAF.

5

6

1



2

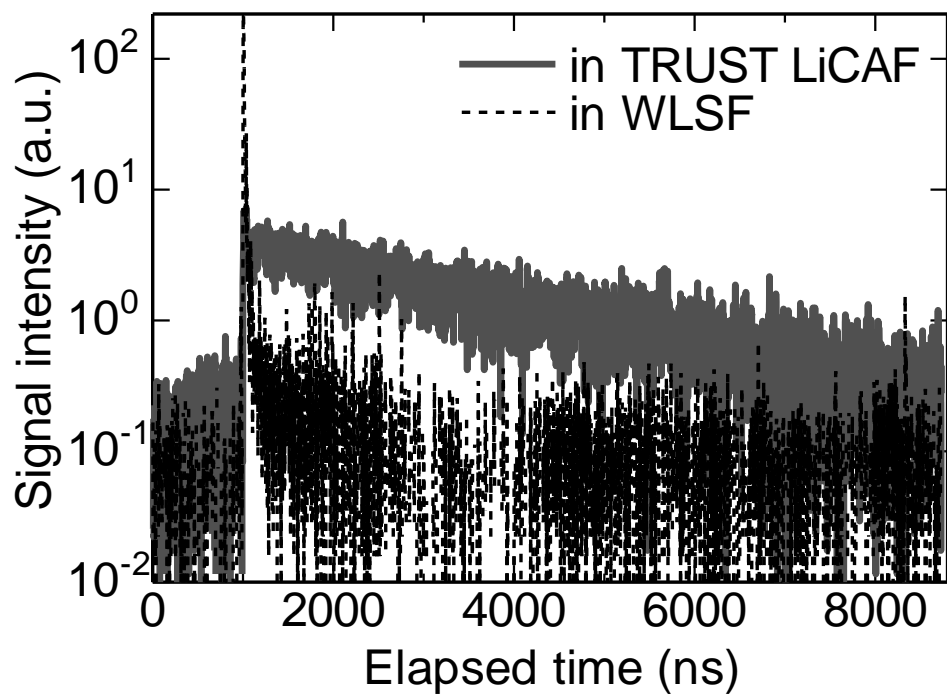
3

4 **Figure 3** Dependence of dosimeter signal intensity on the setting position depth obtained from basic  
5 experiments.

6

7

1



2

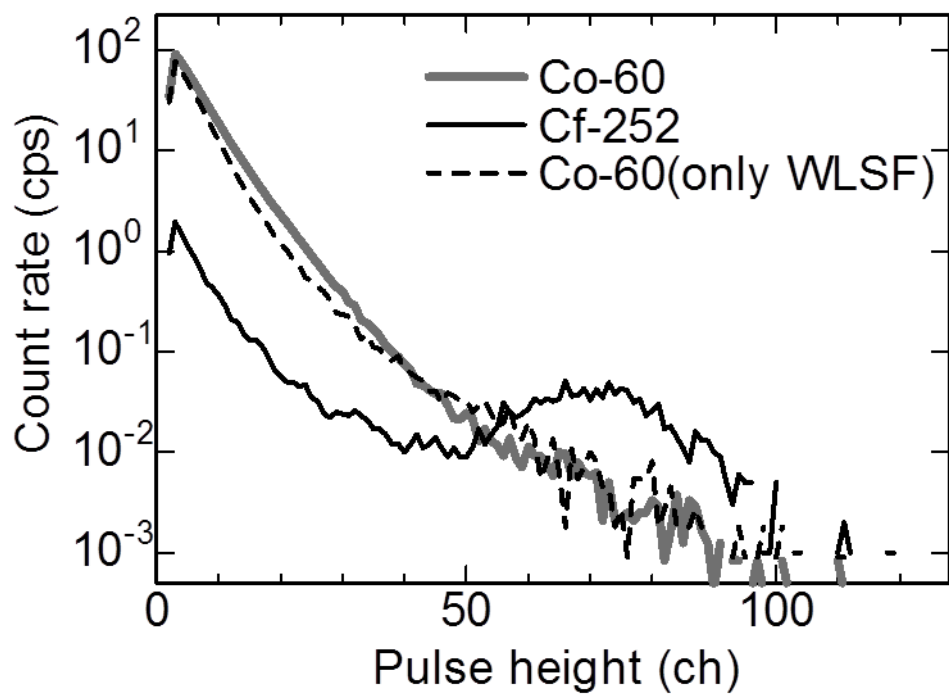
3

4 **Figure 4** Signal waveforms created in the TRUST Eu:LiCAF scintillator and the WLSFs.

5

6

1



2

3

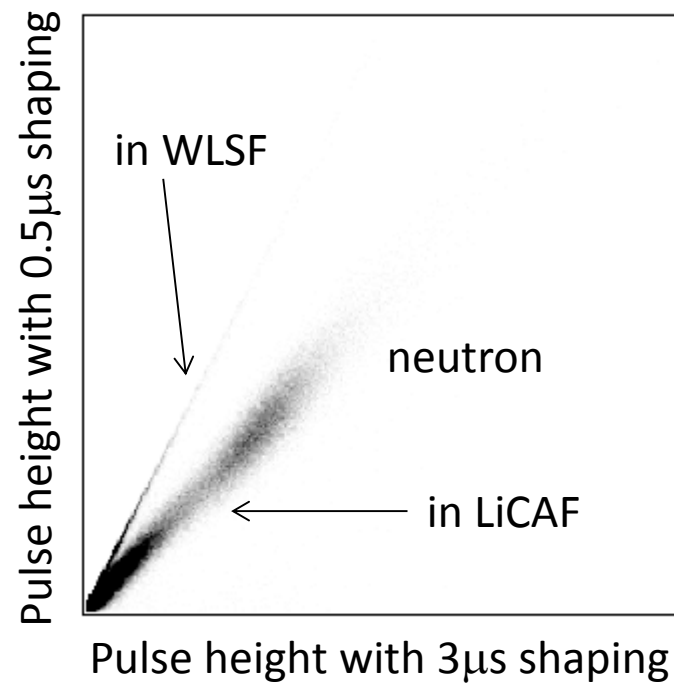
4 **Figure 5** Pulse height spectra obtained from the TRUST Eu:LiCAF scintillator with the WLSF readout.

5

The spectra obtained from only the WLSF plate is also plotted.

6

1



2

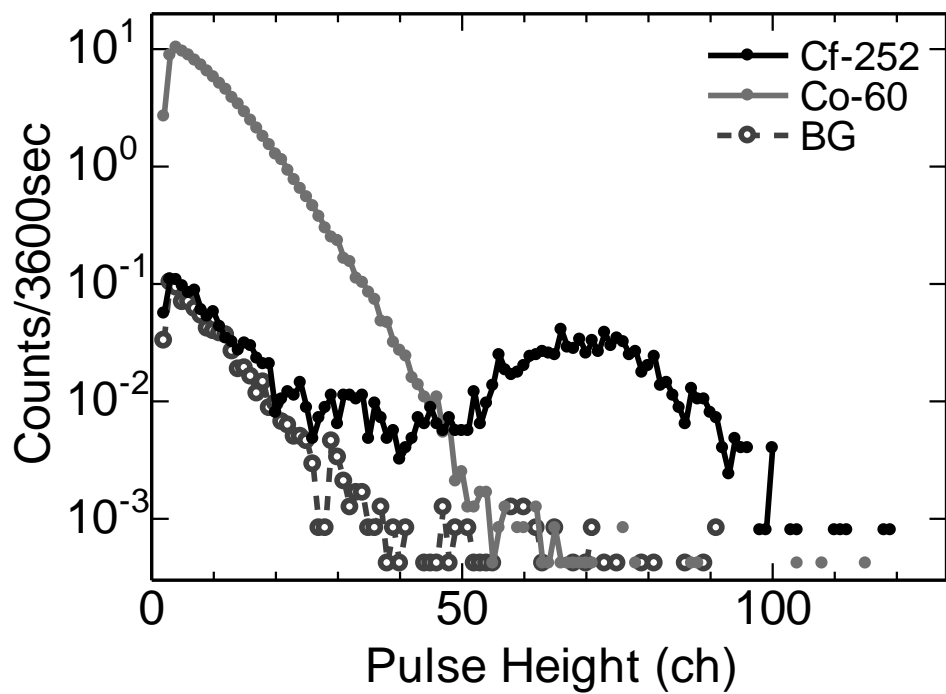
3

4 **Figure 6** Two dimensional histogram between pulse heights of shaped pulses with slow (3  $\mu$ s) and fast (0.5  
5  $\mu$ s) shaping time.

6



1



2

3

4 **Figure 7** Pulse height spectra obtained from the TRUST Eu:LiCAF scintillator with the WLSF readout,  
 5 when applying the pulse shape discrimination.

6